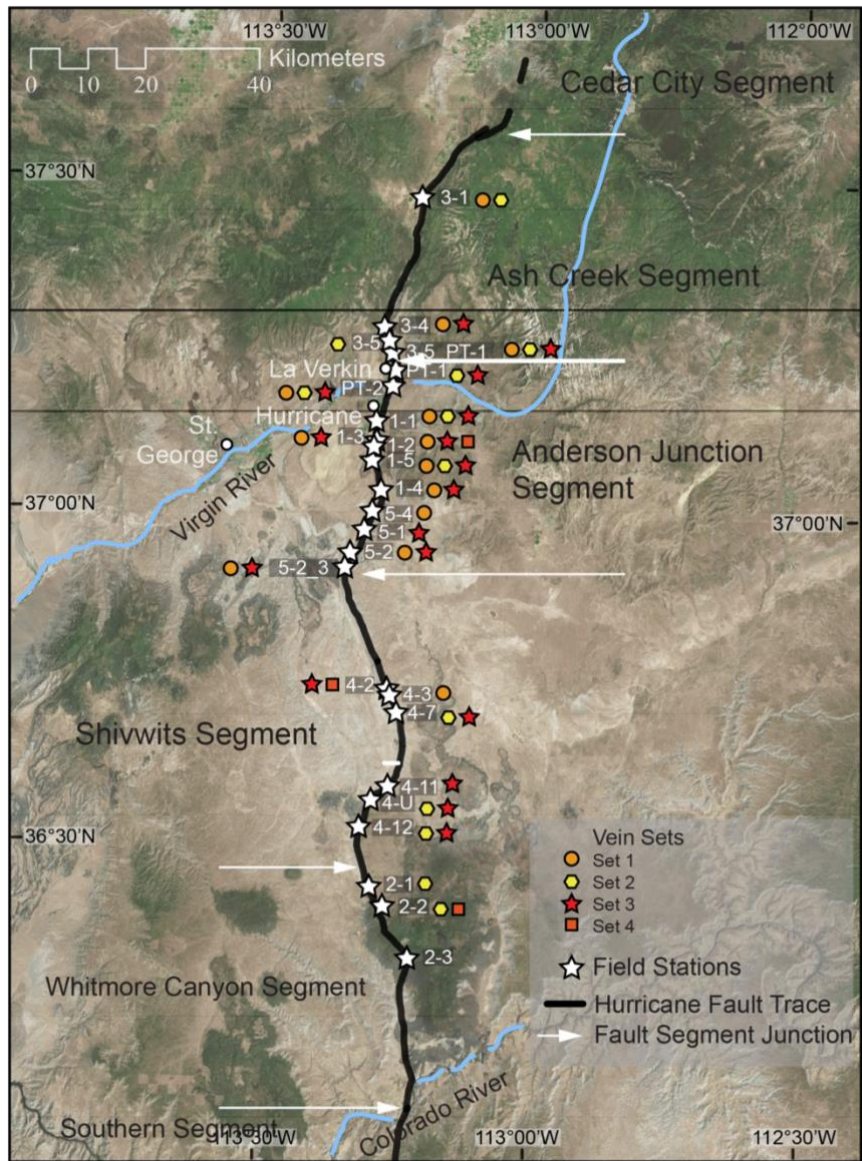


The following supplemental figures, tables, and descriptions support the main manuscript content.

S1. Supplemental geographic and stratigraphic information



5 **Figure S1.** Hurricane fault field stations and observed vein sets. Also shown are the Hurricane Fault segment boundaries. (Image Source: Esri, DigitalGlobe, GeoEye, Earthstar Geographics, CNES/Airbus DS, USDA, USGS, AeroGRID, IGN, and the GIS User Community).

System & Series		Formation	Member	Symbol	THICKNESS meters	LITHOLOGY
Triassic	Upper	Chinle Formation	Petrified Forest Member	Tcp	124-150	
			Shinarump Cgl Mbr	Tcs	35-49	
	Lower	Moenkopi Formation	upper red member	Tmu	120	
			Shnabkaib Member	Tms	120-180	
			middle red member	Tmu	120-150	
			lower red mbr	Tml	60-75	
			Virgin Ls Mbr	Tmv	30	
			Timpoweap Mbr	Tmt	9-40	
			Rock Canyon Cgl	Tmr	0-24	
Permian	Lower	Kaibab Formation	Harrisburg Mbr	Pkh	30-50	
			Fossil Mtn Mbr	Pkf		
		Toroweap Formation	Woods Ranch Mbr	Ptw	40-60	
			Brady Canyon Mbr	Ptb		
			Seligman Mbr	Pts	9-15	
		Hermit Formation	Upper Mbr	Ph	0-60	
			Middle Mbr		0-213	
			Lower Mbr		0-60	
		Queantoweap Sandstone		Pq	300	

Figure S2. Representative stratigraphic column of units exposed in the study area along the trace of the Hurricane Fault (modified from Biek, 2003; Dutson, 2005; Biek et al., 2010).

S2 Hurricane Fault veins and alteration

S2.1 Calcite veins and fracture fills

Various morphologies of veins and fracture coatings are commonly observed features nearby the main fault trace in the footwall damage zone (Fig. S3). Cross-cutting veins at multiple sites indicate that multiple episodes of fracturing and mineralization occurred (Fig. S3 a). Calcite is ubiquitous as a fracture and vein mineral along the Hurricane fault. The majority of veins are composed of sparry calcite, and are particularly common cutting limestone strata (Fig. S3 b). Interconnected, web-like “boxwork” calcite veins are common in sandstone within ~ 50 m of the main fault trace (Fig. S3 c). Other precipitates include manganese oxides, hematite, and gypsum. Intergrown oxide and calcite veins are commonly

20 observed in calcareous sandstone units that contain minor oxide cement (Fig. S3 d, e). The Permian Hermit Formation hosts many of these secondary minerals (e.g., sites 1-4 and 5-2 to 5-3). For example, manganese oxides are observed forming dendrites, associated with calcite veins in sandstone (Fig. S3 e). Although the majority of calcite plus oxide veins are found within sandstone strata, one location (site 1-2) hosts intergrown laminated calcite and minor hematite veins in cherty limestone of the Brady Canyon member of the Toroweap Formation (Fig. S3 f). These veins are located within a ~10-m-wide zone of dense fracturing (~5 m-1). Bands of sparry to fibrous calcite crystals terminate into narrow bands of iron oxide (Fig. 5 b). Gypsum veins are also present and often associated with or stratigraphically near gypsum-rich strata (e.g., site 4-11).

S2.2 Breccia and slip surfaces

Mesoscopic structures associated with fault slip, rock fracture, and alteration along the Hurricane Fault include but are not limited to fault-core breccias, brecciated veins, and striated slip surfaces (Fig. S4). Fault-core breccias along the main trace of the fault are well-exposed in two locations (sites 1-2 and 4-2) between the footwall damage zone and the buried trace of the fault, both hosted in cherty limestone units. These fault-core breccias exhibit grain size reduction of chert clast, and alternating bands of calcite and brecciated host rock (Fig S4 a). Brecciated veins are observed in fine-grained sandstones of the Hermit Formation, particularly at sites 1-4 and 5-2 to 5-3. They are cemented by calcite and minor hematite (Fig. S4 b). Angular clasts are jigsaw-piece shaped and heterogeneous in size, and there is evidence for multiple generations of brecciation and cementation. Cemented breccias are present within zones of relatively high fracture density (≥ 5 m-1) and often associated with redox alteration (e.g., “bleaching”) of the host rock (Fig. S4 c). Striated slip surfaces are common near the main fault trace in the damage zone at numerous study location, particularly those that comprise sandstone host rocks. They are commonly coated by slickenfibres of calcite that vary from <1 mm to multiple cm thick or intergrown calcite and hematite ≤ 2 mm thick (Fig. S4 d). Polished slip surfaces are composed of multiple discrete planes, implying multiple stages of slip.

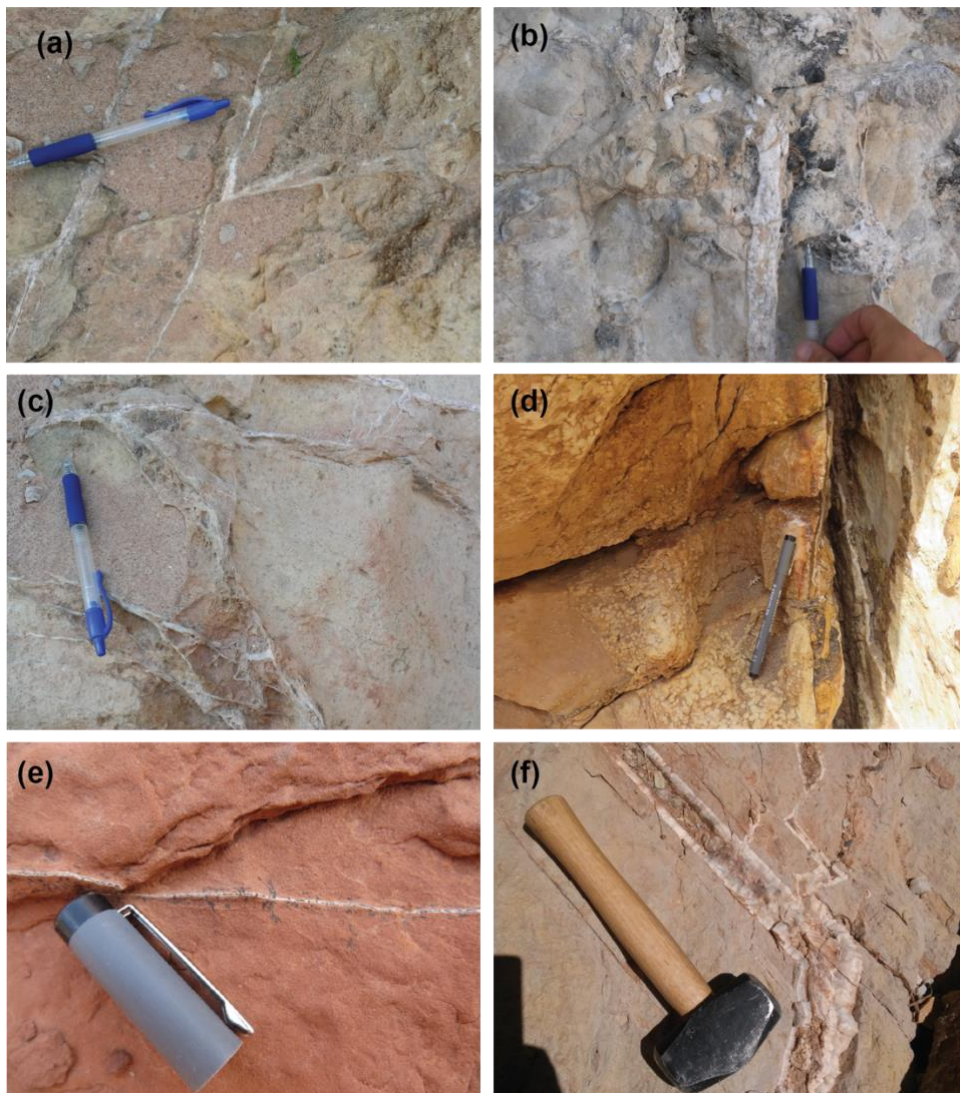


Figure S3. (a) Sets of sparry calcite veins showing offset; (b) Sparry calcite vein in limestone host rock; (c) Boxwork calcite veins; (d) Laminated calcite vein with minor hematite cutting sandstone. Note the small calcite concretions cementing the sandstone parallel to the vein trace; (e) Manganese oxide dendrites associated with mm-scale calcite vein in sandstone; (f) Laminated, cm-scale calcite vein with minor intergrown hematite – cutting cherty limestone host rock.

45

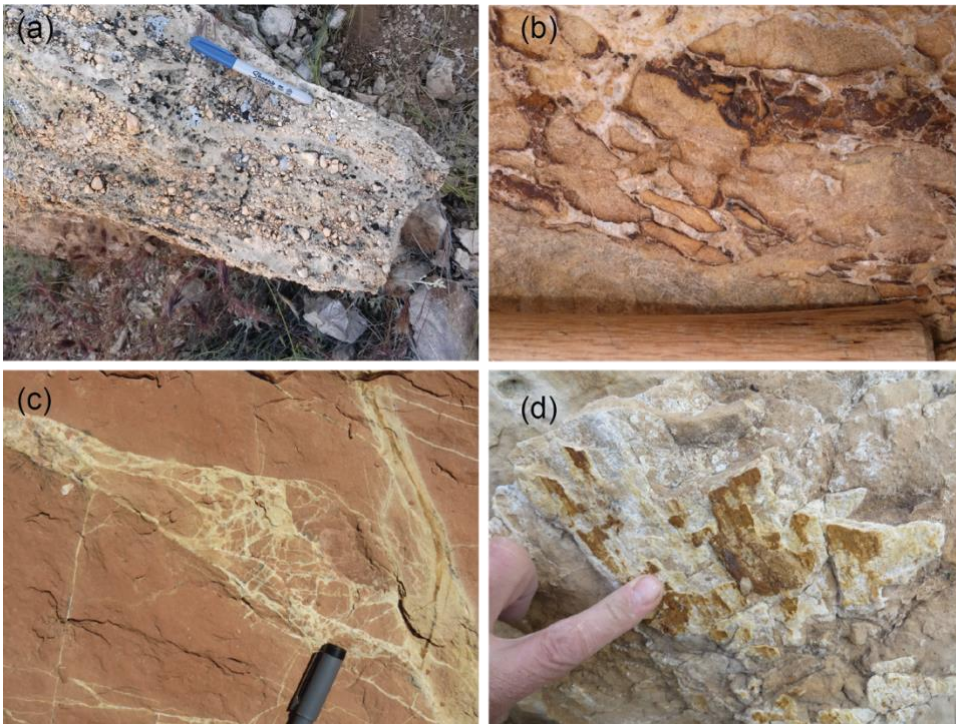


Figure S4. (a) Fault-core breccia in limestone host rock; (b) Calcite and hematite cemented breccia in sandstone host rock (part of rock hammer handle for scale); (c) Brecciated red (hematite cemented) sandstone showing bleaching and minor calcite veining along fractures; (d) Striated fault surfaced with calcite and hematite mineralization

S2.3 Host rock alteration

Where the siliciclastic strata of the Permian Queantoweap Sandstone and Hermit Formation are present in the footwall damage zone, evidence for fluid-rock interaction includes fracture-related redox features and intragranular cements.

Fracture-parallel bands of white to light tan alteration (commonly referred to as bleaching) are found along fault-parallel fractures (Fig. S5 a, b). Bleaching indicates mobilization iron oxide cements in these sandstones. Bleaching halos vary in width with some on the order of 0.1 to 3 cm (Fig. S5 c) and others on the decimeter to meter-scale (Fig. S5 a, b). Alternating stratigraphic horizons are also bleached separated by unaltered strata (Fig. S5 a, c). The degree of sandstone cementation by calcite also changes in the fault zone. Near the fault trace, calcite cementation, including the presence of calcite concretions is greatest adjacent to fractures, and fractures hosting calcite veins (Fig. S3 d).



Figure S5. (a) Looking north along Hurricane Fault trace. Note the offset Permian Queantoweap Sandstone displaying bleaching along the fault trace and in horizontal strata; (b) Decimeter to meter-scale bleached fractures cutting Queantoweap Sandstone; (c) Densely fractured silty sandstone in the Hermit Formation showing mm- to cm-scale bleaching along fractures; (d) Bedding parallel bleaching in Hermit Formation siltstones bounded by unbleached strata.

65

S3 Data table and figure supplements

Table S1. Location of 23 Field Stations along the Hurricane Fault

Field Station	Latitude ^a	Longitude
3-1	37.477510	-113.21409
3-4	37.361312	-113.25263
3-5	37.237774	-113.27133
3-5_PT1	37.227990	-113.25961
PT-1	37.212103	-113.26174
PT-2	37.191258	-113.27319
1-1	37.157048	-113.28758
1-2	37.137324	-113.29661
1-3	37.103990	-113.30294
1-5	37.080825	-113.30608
1-4	37.017787	-113.28893
5-4	36.996654	-113.30263
5-1	36.973909	-113.31452
5-2	36.942954	-113.33335
5-2_3	36.925742	-113.35111
4-2	36.725976	-113.26352
4-3	36.714396	-113.25492
4-7	36.695012	-113.24731
4-11	36.580715	-113.28505
4-U	36.569903	-113.29930
4-12	36.519993	-113.31926
2-1	36.443720	-113.29808
2-2	36.421994	-113.28260

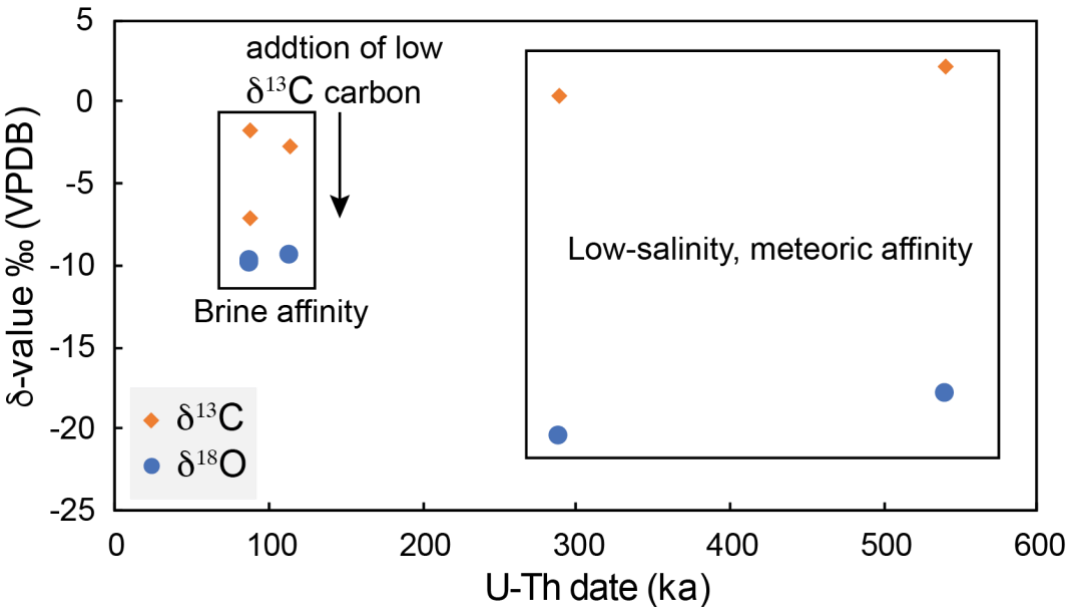
^a WGS 84 datum

Table S2. U-Th data for the 5 calcite veins. All ratios are activity ratios.

Sample ID	$^{230}\text{Th}/^{238}\text{U}_{\text{truea}}$	$^{234}\text{U}/^{238}\text{U}_{\text{true}}$	$^{230}\text{Th}/^{232}\text{Th}_{\text{true}}$	$^{232}\text{Th}/^{238}\text{U}_{\text{true}}$	$\delta^{235}\text{U}_{\text{rel to CRM145}}$	$\delta^{235}\text{U}_{\text{stds rel to CRM145}}$	age (y) ^b	$^{234}\text{U}/^{238}\text{U}_{\text{init}}$
JK15HR110	0.9373	1.007	1510	6.21E-04	0.0		287,856 ± 5757	
JK15HR111	0.8306 ± 0.0008	1.469 ± 0.002	588±1.23	1.41E-03 ± 2.85E-06	-0.3±0.2	-0.3±0.3	85,993 ± 196	1.598 ± 0.004
JK15HR103	1.1609	1.120	87	1.33E-02	-0.1		539,304 ± 10786	
JK15HR27	0.9437 ± 0.0009	1.403 ± 0.002	240±0.503	3.94E-03 ± 7.95E-06	0.5±0.	0.0±0.3	113,062 ± 315	1.555 ± 0.004
JK15HR35	0.8110	1.435	422	1.92E-03	0.0		86,233± 1725	

^a Where reported, errors are 1-sigma. Due to slight method differences, these errors are not available for all samples

^b Errors for JK15HR110 and 103 are estimated as 2%, rather than 1-sigma due to method differences



80 **Figure S6. Carbon and oxygen stable isotope values and corresponding U-Th dates for the 5 dated samples. The likely fluid-endmember is identified based on stable isotope values.**

References Cited

Biek, R.: Geologic Map of the Hurricane Quadrangle Washington County, Utah: Utah Geological Survey Map, 187, 2003.

Biek, R., Rowley, P., Hayden, J., Hacker, D., Willis, G., Hintze, L., Anderson, R., and Brown, K.: Geologic map of the St. George and east part of the Clover Mountains 30'X60' quadrangles, Washington and Iron counties, Utah, Utah Geological Society, 2010.

85 Dutson, S.: Effects of Hurricane Fault Architecture on Groundwater Flow in the Timpoweap Canyon of Southwestern, Utah [MS thesis]: Provo, Brigham Young University, 2005.